

Organic Molecules in Low-Mass Protostellar Hot Cores: Submillimeter Imaging of IRAS 16293-2422

Yi-Jehng Kuan^{1,2}, Hui-Chun Huang¹, Steven B. Charnley³,
Naomi Hirano², Shigehisa Takakuwa⁴, David J. Wilner⁵, Sheng-Yuan Liu²,
Nagayoshi Ohashi², Tyler L. Bourke⁴, Chunhua Qi⁵, Qizhou Zhang⁵

ABSTRACT

Arcsecond-resolution spectral observations toward the protobinary system IRAS 16293-2422 at 344 and 354 GHz were conducted using the Submillimeter Array. Complex organic molecules such as CH₃OH and HCOOCH₃ were detected. Together with the rich organic inventory revealed, it clearly indicates the existence of two, rather than one, compact *hot molecular cores* ($\lesssim 400$ AU in radius) associated with each of the protobinary components identified by their dust continuum emission in the inner star-forming core.

Subject headings: astrochemistry—ISM: abundances—ISM: individual (IRAS 16293-2422)—ISM: molecules—radio lines: ISM—stars: formation

1. Introduction

The low-mass protostellar source IRAS 16293-2422 (hereafter I16293) is located in the ρ Ophiuchus cloud complex at a distance 160 pc from the Sun. High angular-resolution observations revealed that I16293 is also a protobinary system of two components with

¹Department of Earth Sciences, National Taiwan Normal University, 88 Sec.4 Ting-Chou Rd., Taipei 116, Taiwan, Republic of China; kuan, hspring@sgrb2.geos.ntnu.edu.tw

²Academia Sinica Institute of Astronomy & Astrophysics, P. O. Box 23-141, Taipei 106, Taiwan, ROC; hirano, ohashi, syliu@asiaa.sinica.edu.tw

³Space Science Division, MS 245-3, NASA Ames Research Center, Moffett Field, CA 94035; charnley@dusty.arc.nasa.gov

⁴Harvard-Smithsonian Center for Astrophysics, Submillimeter Array Project, 645 N. A'ohoku Place, Hilo, HI 96721; stakakuw@sma.hawaii.edu

⁵Harvard-Smithsonian Center for Astrophysics, 60 Garden Street, Cambridge, MA 02138; dwilner, tbourke, cqi, qzhang@cfa.harvard.edu

a projected separation of $\sim 5.2''$ (~ 840 AU), and 3-mm continuum observations (Looney, Mundy & Welch 2000) suggest that the northwest component ($0.61 M_{\odot}$, hereafter I16293B) is slightly more massive than the southeast component ($0.49 M_{\odot}$, hereafter I16293A). Single-dish submillimeter line-surveys led van Dishoeck *et al.* (1995) to conclude that, within a $20''$ region, I16293 consists of a cold ($T_{\text{kin}} \simeq 10\text{--}20$ K) outer molecular envelope, a warmer ($T_{\text{kin}} \simeq 40$ K) circumbinary envelope of $10''\text{--}15''$ in size, and a hot ($T_{\text{kin}} \gtrsim 80$ K) region of dense gas only $3''\text{--}10''$ in size. This innermost gas was found to be rich in organic molecules and it was suggested that their presence was due to outflows (Hirano *et al.* 2001) interacting with the circumbinary envelope. However, Ceccarelli *et al.* (1999, 2000) showed that the emitting region is warm (100 K), dense $n_{\text{H}_2} \gtrsim 10^7 \text{ cm}^{-3}$, and very compact ($\sim 2''\text{--}3''$). This led to the suggestion that I16293 contained a *hot molecular core* about 150 AU in size where high dust temperatures ($T_{\text{dust}} \gtrsim 100$ K) can facilitate the evaporation of icy grain mantles (Ceccarelli *et al.* 2000). This conclusion is supported by recent observations which show that I16293 *inner* hot core has a molecular inventory rich in complex molecules, similar to the hot molecular cores (HMCs) associated with massive protostars (Cazaux *et al.* 2003).

Nevertheless, several questions remain that cannot easily be answered by single-dish observations. One major concern is that its inferred size of ~ 150 AU ($\lesssim 1''$) (Ceccarelli *et al.* 2000; Schöier *et al.* 2002) is much smaller than the binary separation in I16293, and comparable to the dimensions of protostellar disks. Furthermore, it is unknown whether high resolution observations of low-mass hot cores will exhibit clear chemical differentiation on small spatial scales, similar to that seen in massive HMCs (e.g. Wyrowski *et al.* 1997).

Submillimeter Array⁶ observations with arcsecond resolution ($1''=160$ AU) were carried out on 2003 March 14 (compact configuration) and July 12 (extended configuration) with 5 antennae. The phase tracking center of the observations was $\alpha(\text{J2000}) = 16^{\text{h}}32^{\text{m}}22^{\text{s}}.91$, $\delta(\text{J2000}) = -24^{\circ}28'35''.52$. The digital correlator at the time was configured with eight overlapping segments ("chunks") each of 104 MHz bandwidth and 128 channels, except one chunk which had 512 channels, giving a frequency resolution of 0.812 and 0.203 MHz, respectively. The total bandwidth of each sideband was ~ 670 MHz covering two frequency ranges: 343.555–344.225 GHz (LSB) and 354.211–354.881 GHz (USB). Quasars 1743-038 and NRAO530 were observed for phase and amplitude calibration. The flux scale is estimated to be accurate to 25%. The synthesized beam sizes are $\sim 1''.3 \times 2''.7$ at 344 GHz and $\sim 1''.1 \times 2''.5$ at 354 GHz with natural weighting; these beams correspond to a linear scale of $\sim 200 \times 400$ AU at a distance of 160 pc. The data were calibrated using the MIR software,

⁶The Submillimeter Array is a joint project between the Smithsonian Astrophysical Observatory and the Academia Sinica Institute of Astronomy and Astrophysics, and is funded by the Smithsonian Institution and the Academia Sinica

and imaging was done with MIRIAD software.

2. Results and Discussions

To make positive identifications of the spectral features detected, in addition to the basic requirement of frequency coincidence, an iterative process with the following stringent selection criteria was applied to each candidate species: 1). Expected line intensity - unfavorably weak transitions were rejected. 2). Looking for transitions with similar or stronger line intensities in the bands - if missing, the particular candidate line was excluded. 3). Looking for slightly less favored transitions of the same molecule for a possible sign of low-level ($< 3\sigma$) "detections" if no other stronger transitions predicted were available in the bands. This would be an indirect verification of the particular line identified. 4). Literature check against lists of known molecules in I16293 in the literature - not mandatory for a detection as SMA is sensitive to dense hot cores. 5). Making the requirement that the molecular candidate has to be a known hot core molecule.

Table 1 lists some of the representative molecular transitions detected. The LSR velocity of each molecular line measured is also listed in Table 1. Single-dish observations reveal that the LSR velocity of I16293 is centered at 3.9 to 4.2 km s⁻¹ and is often found within the range of 3.3–4.7 km s⁻¹. Asymmetric double-peak line profiles with the blueshifted peak at 2.5–3.5 km s⁻¹ and the red one at 5.0–6.0 km s⁻¹ are readily seen in single-dish observations.

On the other hand, an interferometer like the SMA can easily filter out the diffuse ambient cloud, such as the warm gas envelope of I16293 at $V_{\text{LSR}} \sim 3.9\text{--}4.2$ km s⁻¹, and its small beam will tend to pick up the fine kinematic details of dense hot regions. The SMA beam is small enough to resolve the two protobinary components in I16293, thus SMA is able to trace individual velocity component in the rotating disks and/or hot cores. As shown in Fig. 1a, the two protobinary components are clearly resolved in the continuum emission. Sample images of five organic molecules are shown in Figs. 1b-f. Fig. 2 shows the sample spectra of four large organic molecules plus HC¹⁵N in I16293A and I16293B. By examining HC¹⁵N emission toward I16293A, two major velocity components, one at 1.7 km s⁻¹ and the other at 4.7 km s⁻¹ were seen (Fig. 2a); in I16293B, one component at 2.5 and the other at 6.0 km s⁻¹ were also exhibited (Fig. 2b). Furthermore, the small beam of an array suffers less beam dilution, thus is sensitive to high-velocity components within compact sources. In the case of HCN 4–3 and HC¹⁵N, for example, linewidths $\gtrsim 8$ km s⁻¹ are seen toward I16293A. The HCOOCH₃ line in I16293A is also fairly wide, with a linewidth of ~ 8 km s⁻¹ (Fig. 2e). The large linewidth (5–8 km s⁻¹) is common for simple molecules like HCN, or strong molecular emission like HC₃N and CH₃OH. For weaker emission, typical linewidths

are of 2–4 km s^{−1} in I16293A; however, toward I16293B, the linewidths of most molecular lines are notably narrower, i.e., between 2 and 4 km s^{−1}.

Because of array characteristics and sensitivity, it is not unusual that an array can preferentially pick up only the stronger emission peak of a double-peak profile as seen by a single-dish. The CH₃OH line shows $V_{\text{LSR}} \sim 2.5$ km s^{−1} toward I16293A, with two velocity components visible near 4.6 and 1.8 km s^{−1} (Fig. 2c). The kinematic structure traced is thus similar to what seen by HC¹⁵N; a similar line profile of ¹³CH₃OH was also observed toward I16293A. Toward I16293B, the CH₃OH emission is weaker and is mainly from the blueshifted component near 2.5 km s^{−1} (Fig. 2d), which again agrees well with what was seen by HC¹⁵N. Since the optically thin HC¹⁵N emission basically traced the densest regions such as the disks, it suggests methanol may also reside in the same dense regions. However, it is also plausible that the two velocity components seen in the methanol line profile are due to self absorption at ~ 3.9 km s^{−1}. Toward I16293B, the LSR velocities of HCOOCH₃ lines were found consistent with each other at ~ 3.9 km s^{−1}, within the velocity uncertainty of ~ 0.7 km s^{−1}. However, a non-trivial velocity scattering with V_{LSR} between 3.9 and 6.0 km s^{−1} was observed toward I16293A. A close examination of the integrated intensity maps of HCOOCH₃ show their peak emission positions are situated at $\sim 0''.5$ east ($V_{\text{LSR}} = 3.9$ km s^{−1}) and south ($V_{\text{LSR}} = 5.9$ and 6.0 km s^{−1}) of the I16293A center position where $V_{\text{LSR}} \sim 4.6$ km s^{−1}. Again, such a velocity field variation traces the general velocity gradient seen by the HC¹⁵N emission nicely.

All spectral emission appears to originate from two compact regions of a beam-convolved size of $\sim 200 \times 400$ AU in radius, concentrated toward the two protobinary components I16293A and I16293B. An exception is the 4–3 HCN transition which shows complicated kinematic structure (Takakuwa *et al.* 2004, in preparation).

The beam-averaged line-of-sight column densities and fractional abundances of all observed molecules are listed in Table 2, where a gas column density $N_{\text{H}_2} = 1.6 \times 10^{24}$ cm^{−2} (Schöier *et al.* 2002) was adopted for both protostellar cores. Column densities were measured at the peak emission positions of each integrated spectral line and were derived assuming thermalized level populations and optically thin lines. At these high densities, gas and dust are expected to be thermally well-coupled and so an excitation temperature $T_{\text{ex}} \simeq T_{\text{dust}} = 100$ K was adopted, except for molecular transitions with energy levels > 500 cm^{−1} ($\gtrsim 700$ K) where $T_{\text{ex}} = 300$ K was used (Schöier *et al.* 2002). For HCOOCH₃, with multi-line detections, the column densities were derived from rotation diagrams (Fig. 3); we found $T_{\text{ex}} = 105$ K for I16293A, and 116 K for I16293B. The assumption of $T_{\text{ex}} = 100$ K applied for transitions of lower energy levels is hence warranted.

The derived fractional abundances and relative column densities are in good agreement

with those derived from submillimeter observations of the Orion KL and Sgr B2 massive HMCs (Sutton *et al.* 1991, 1995). When molecular emission is mainly from the compact cores, abundances derived using the smaller SMA beam can be much higher (e.g. *c*-C₃H₂) than found in previous single-dish observations (van Dishoeck *et al.* 1995; Cazaux *et al.* 2003). This explains why CH₃OH abundances derived from modeling higher energy transitions (Schöier *et al.* 2002) in the *inner* I16293 core show good agreement with our values, and suggests that the lower array abundances for HCN and HCOOCH₃ is indicative of less compact emission where the extended component is filtered out by the interferometer.

The high abundances of organic molecules, particularly methanol, indicates that icy mantles have recently been evaporated (Charnley, Tielens & Millar 1992). For many molecules detected in both sources, the measured abundances only differ by factors of about 2–3; as expected if both cores collapsed from the same cold core material. Nevertheless, the apparent absence of *c*-C₃H₂ and CH₂CO in I16293A, if confirmed, raises the prospect that future observations could discover pronounced chemical differentiation between the two cores.

We have resolved the hot cores surrounding both protostellar sources in I16293 and measured the chemical composition in each. These preliminary observations demonstrate that the SMA will be an important tool to further explore the connection between the volatile organic chemical composition of the hot cores associated with massive protostars, those of Solar mass, and the composition of comets.

This work was supported by NSC 92-2112-M-003-006 grant (Y.-J.K.) and by NASA’s Exobiology and Origins of Solar Systems Programs through NASA Ames Cooperative Agreement No. NCC2-1412 (S.B.C.).

REFERENCES

- Cazaux, S., Tielens, A.G.G.M., Ceccarelli, C., Castets, A., Wakelam, V., Caux, E., Parise, B., & Teyssier, D. 2003, *ApJ*, 593, L51
- Ceccarelli, C., *et al.* 1999, *A&A*, 342, L21
- Ceccarelli, C., Loinard, L., Castets, A., Tielens, A.G.G.M., & Caux, E. 2000, *A&A*, 357, L9
- Charnley, S.B., Tielens, A.G.G.M., & Millar, T.J. 1992, *ApJ*, 399, L71
- Hirano, N., Mikami, H., Umemoto, T., Yamamoto, S., & Taniguchi, Y. 2001, *ApJ*, 547, 899

- Looney, L.W., Mundy, L.G., & Welch, W.J. 2000, *ApJ*, 529, 477
- Schöier, F.L., Jørgensen, J.K., van Dishoeck, E.F., Blake, G.A. 2002, *A&A*, 390, 1001
- Sutton, E.C., Jaminet, P.A., Danchi, W.C., Blake, G.A. 1991, *ApJS*, 77, 255
- Sutton, E.C., Peng, R., Danchi, W.C., Jaminet, P.A., Sandell, G., & Russell, A.P.G. 1995, *ApJS*, 97, 455
- van Dishoeck, E.F., Blake, G.A., Jansen, D.J., & Groesbeck, T.D. 1995, *ApJ*, 447, 760
- Wyrowski, F., Hofner, P., Schilke, P., Walmsley, C.M., Wilner, D.J., & Wink, J.E. 1997, *A&A*, 320, L17

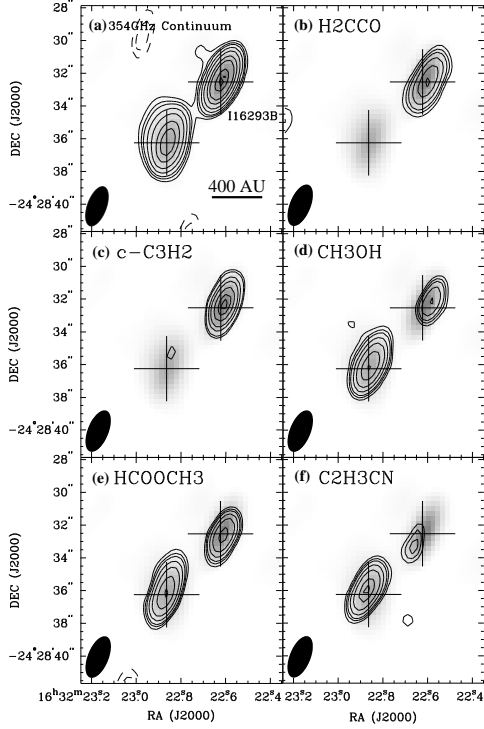


Fig. 1.— Spectral images of large organic molecules toward I16293. (a) Continuum at 354 GHz; (b) spectral emission of CH_2CO ; (c) $c\text{-C}_3\text{H}_2$ emission; (d) CH_3OH ; (e) HCOOCH_3 at 344029 MHz; and (f) CH_2CHCN . Crosses mark the positions of I16293A and I16293B hot cores. The angular size for a linear scale of 400 AU is shown in (a). The grey scale denotes the 354 GHz continuum. Continuum emission was imaged with the wide continuum channel at 354 GHz, at a noise level of $0.11 \text{ Jy beam}^{-1}$, and the estimated line contamination is $< 3\%$ in I16293A and $< 1\%$ in I16293B. The continuum flux density of I16293A is $4.97 \pm 0.49 \text{ Jy}$, which is slightly lower than that of I16293B ($5.14 \pm 0.61 \text{ Jy}$). The dark ellipse represents the HPBW of the synthesized beam. Contours are shown at 3-, 4-, 5-, 7- σ levels in general, then at irregular intervals up to the peak values; dashed lines indicate contours at negative 3- and 4- σ levels.

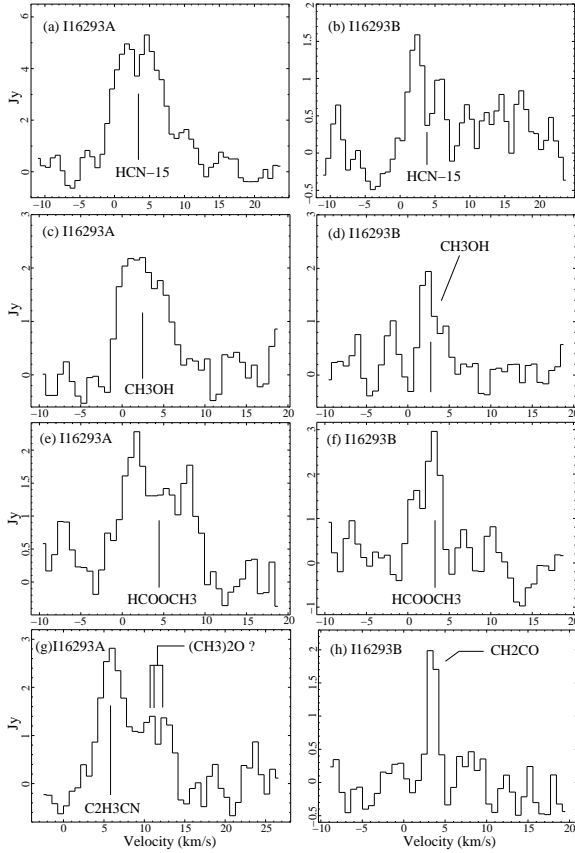


Fig. 2.— Sample spectra of large organic molecules toward I16293. The left column shows spectra taken at I16293A; the right column, at I16293B. HC^{15}N spectra are shown in (a) and (b); CH_3OH , in (c) and (d); and HCOOCH_3 (344029 MHz), in (e) and (f). (g) gives $\text{C}_2\text{H}_3\text{CN}$ line and (h), CH_2CO . Tentatively detected $(\text{CH}_3)_2\text{O}$ $17_{2,16}$ - $16_{1,15}$ EA, AE, EE & AA transitions at 343753.3, 343754.2 and 343755.1 MHz can also be seen in (g). The weaker spectral appearance of the tentative $(\text{CH}_3)_2\text{O}$ line is because spectrum (g) is taken at the peak position of the integrated CH_2CHCN line. All spectra were Hanning smoothed for better S/N ratios.

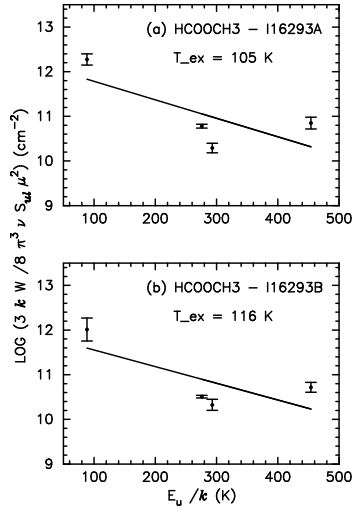


Fig. 3.— The rotation diagrams of HCOOCH₃. Note that the 344170 MHz doublet ($E_u = 454 \text{ K}$) appears to be situated at a location slightly higher in the rotation-diagram fits. It might imply this doublet is just in the transitional regime toward a higher excitation, or it might indicate simply this is a misidentified line. Excluding this doublet would result in a lower excitation temperature, which agrees better with the value ($\sim 60 \text{ K}$) of Cazaux *et al.* (2003).

Table 1. Sample molecules detected toward IRAS 16293-2422 protostellar cores.

Molecule	Transition	Frequency (MHz)	E_{low} (cm ⁻¹)	$I_{\nu,16293A}$ ^a (Jy beam ⁻¹)	$V_{LSR,A}$ ^b (km s ⁻¹)	$I_{\nu,16293B}$ ^a (Jy beam ⁻¹)	$V_{LSR,B}$ ^b (km s ⁻¹)
HCN	4-3	354505.5	17.7	10.88±0.44	4.6	9.92±0.44	3.6
HC ¹⁵ N	4-3	344200.3	17.2	5.26±0.24	3.9	1.72±0.24	3.9
<i>c</i> -C ₃ H ₂	23 _{13,10} -23 _{12,11}	343804.9	548.9	2- σ ^c	...	3.48±0.32	4.6
CH ₂ CO	17 _{2,15} -16 _{2,14}	343693.9	127.9	2- σ	...	1.98±0.28	3.5
HC ₃ N	39-38	354697.4	224.8	3.30±0.20	4.6	1.54±0.20	3.9
CH ₃ OH	18 _{2,16} -17 _{3,14} E	344109.1	280.0	2.20±0.15	2.5	1.94±0.15	2.5
¹³ CH ₃ OH	4 _{1,3} -3 _{0,3} A	354445.9	18.6	2.27±0.20 ^d	2.5	2- σ	...
C ₂ H ₃ CN (<i>v</i> ₁₅ =1)	36 _{4,32} -35 _{4,31}	343761.8	564.9	2.82±0.26	5.3	0.94±0.26	5.3
HCOOCH ₃	32 _{*,32} -31 _{*,31} A	344029.6 ^e	180.4	2.28±0.16	4.6	2.96±0.16	3.2
	32 _{2,31} -31 _{1,31} E	344029.8 ^f	180.4				
	28 _{18,10} -27 _{18,9} A	344170.9	304.2	1.09±0.20	6.0	1.04±0.20	3.9
	28 _{18,11} -27 _{18,10} A	344170.9	304.2				
	33 _{*,33} -32 _{*,32} A	354608.0 ^e	191.9	1.71±0.20	5.9	2.75±0.20	3.9
	33 _{2,32} -32 _{1,32} E	354608.4 ^g	191.9				
	12 _{8,5} -11 _{7,5} E	354742.4	49.7	1.85±0.19	3.9	0.98±0.19	3.9

^a The line intensity measured in Hanning-smoothed spectrum at the peak-emission position of integrated intensity map. This value is generally lower than the actual peak intensity shown in channel maps due to Hanning smooth.

^b The uncertainty of the LSR velocity determined is ~ 0.7 km s⁻¹.

^c Only a ~ 2 - σ ($\lesssim 0.6$ Jy beam⁻¹) detection in channel maps.

^d Partially blended with weak HCOOH *b*-type transition 17_{0,17}-16_{1,16} at 354448.3 MHz.

^e * = 0, 1.

^f Together with transitions 32_{1,32}-31_{1,31} E, 32_{2,31}-31_{2,30} E and 32_{1,32}-31_{2,30} E.

^g Together with transitions 33_{1,33}-32_{1,32} E, 33_{2,32}-32_{2,31} E and 33_{1,33}-32_{2,31} E.

Table 2. Molecular column densities and fractional abundances toward IRAS 16293-2422.

Molecule	I16293A			I16293B			HMC	IRAS 16293
	$\int I_\nu dV^a$	N^b (cm^{-2})	X (N/N_{H_2})	$\int I_\nu dV^a$	N^b (cm^{-2})	X (N/N_{H_2})	X (N/N_{H_2})	X (N/N_{H_2})
HCN	91.80	3.1(+14)	2.0(-10)	49.03	1.7(+14)	1.0(-10)	3.2(-9) ^c	1.9(-9) ^d
HC ¹⁵ N	42.86	1.2(+14)	7.4(-11)	6.97	1.9(+13)	1.2(-11)	...	7.0(-12) ^d
<i>c</i> -C ₃ H ₂	10.03	7.2(+15) ^e	4.5(-9)	6.3(-11) ^c	3.5(-11) ^d
CH ₂ CO	3.22	1.9(+15)	1.2(-9)	3.(-10) ^f	1.8(-10) ^d , 5.0(-8) ^g
HC ₃ N	16.73	6.7(+14)	4.2(-10)	3.34	1.3(+14)	8.4(-11)	1.8(-9) ^f	2.5(-11) ^d , 1.0(-9) ^g
CH ₃ OH	13.62	1.1(+18)	6.8(-7)	6.20	5.0(+17)	3.1(-7)	1.4(-7) ^f	4.4(-9) ^d , 3.0(-7) ^g
¹³ CH ₃ OH	17.03	8.1(+16)	5.0(-8)
CH ₂ CHCN	8.58	1.5(+16) ^e	9.4(-9)	2.35	4.1(+15) ^e	2.6(-9)	1.5(-9) ^f	...
HCOOCH ₃	— ^h	6.8(+15)	4.3(-9)	— ^h	4.2(+15)	2.6(-9)	1.4(-8) ^f	2(-7) ⁱ

^a In Jy $\text{bm}^{-1} \text{km s}^{-1}$.

^b $T_{\text{ex}} = 100 \text{ K}$ was assumed for all lines except where noted. For HCOOCH₃, column densities were derived from actual rotation-diagram fits.

^c Sgr B2(M) hot core; from Sutton *et al.* (1991).

^d Single-dish observations with a $\sim 20''$ beam; from van Dishoeck *et al.* (1995).

^e For transitions with energy levels $> 500 \text{ cm}^{-1}$, $T_{\text{ex}} = 300 \text{ K}$ is adopted.

^f Orion KL hot core; from Sutton *et al.* (1995).

^g IRAS 16293 hot core; from models of Schöier *et al.* (2002).

^h In I16293B, the integrated intensities of HCOOCH₃ lines are 8.71, 3.14, 5.55 and 2.31 Jy $\text{bm}^{-1} \text{km s}^{-1}$ with increasing frequency, and in I16293A, 16.22, 4.25, 5.12 and 4.22 Jy $\text{bm}^{-1} \text{km s}^{-1}$.

ⁱ Single-dish observations with $\sim 10'' - 30''$ beam; from Cazaux *et al.* (2003).